Physica Scripta



RECEIVED 5 October 2023

5 October 2025

REVISED

22 December 2023

ACCEPTED FOR PUBLICATION

4 January 2024

PUBLISHED 15 January 2024

PAPER

Effects of size mismatch of halide ions on the phase stability of mixed halide perovskites

Fuqian Yang

Materials Program, Department of Chemical and Materials Engineering, University of Kentucky, Lexington, KY 40506, United States of America

E-mail: fyang2@uky.edu

Keywords: size mismatch, strain energy, Gibbs free energy, phase stability, mixed halide perovskite

Abstract

The phase stability of mixed halide perovskites plays a vital role in the performance and reliability of perovskite-based devices and systems. In this work, we incorporate the contribution of the strain energy due to the size mismatch of halideions in Gibbs free energy for the analysis of the phase stability of mixed halide perovskites. Analytical expressions of the chemical potentials of halide ions in mixed halide perovskites are derived and used to determine the critical atomic fractions of halide ions for the presence of spinodal decomposition (phase instability). The numerical analysis of CH₃NH₃PbI_xBr_{3-x} mixed halide perovskite reveals the important role of the mismatch strain from halide ions in controlling the phase instability of mixed halide perovskite, i.e., increasing the mismatch strain widens the range of x for the phase separation of mixed halide perovskites. To mitigate the phase instability associated with the strain energy from intrinsic size mismatch and/or light-induced expansion, strain and/or field engineering, such as high pressure, can be likely applied to introduce strain and/or field gradient to counterbalance the strain gradient by the mismatch strain and/or light-induced expansion.

Introduction

The progress in the solution-based synthesis of inorganic and organic—inorganic halide perovskites on the nanoand microscales has stimulated the interests for the applications of halide perovskites in optoelectronics [1–5] and bioimaging [6–9]. In the heart of the interests in a variety of applications is the tunability of the optoelectronic characteristics of halide perovskites with high coefficients of optical absorption, low binding energies of excitons, and long-range diffusion of carriers. The power conversion efficiency of more than 20% for perovskite-based solar cells has been reached [10–12], comparable to Si-based solar cells. However, one of the challenges in the commercialization of perovskite-based solar cells is the structural deterioration of perovskite films (layers) associated with the phase separation/segregation and diffusion of halogen atoms (Cl, Br and I) presented in the perovskite films under electric field and photo irradiation, which limits the prospects in the applications of tandem solar cells and light-emitting diodes.

Vashishtha and Halpert [13] reported phase separation in CsPbBr_{3-y}I_y nanocrystals under electric field and red shift and peak splitting for electroluminescence. Zhang *et al* [14] observed that inorganic mixed-halide perovskite nanocrystals experienced blue shift of the emission light under laser irradiation in contrast to red shift reported in the literature and attributed to the effects of the migration of halogen elements. Elmelund *et al* [15] examined photo-induced segregation of halide ions in the mixture of organic halide perovskites and observed linear dependence between the excitation intensity threshold and the heating temperature. Knight *et al* [16] investigated the separation of ions in the films made from the mixture of MAPb(Br_{0.5}I_{0.5})₃ (MA⁺ = CH₃NH₃⁺, methylammonium,) and FA_{0.83}Cs_{0.17}Pb(Br_{0.4}I_{0.6})₃ (FA = CH(NH₂)⁺₂, formamidinium) and suggested the presence of fast paths for ionic migration similar to grain boundary diffusion. In general, the phase separation in hybrid perovskites is associated with the segregation of halide ions in a range of halide ratios. For example, MAPb(Br_vI_{1-y})₃ exhibits the segregation of halide ions for *y* in a range of 0.2 to 1 [17–20]. Brivio *et al* [21] used

Figure 1. (a) Formation of $CsPbI_2Br$ with its crystal structure from the CIF file (ID: 8000558) of Crystallography Open Database and the references of [29, 30], and (b) schematic for the formation of X_3Y from X and Y.

first-principles total energy calculations and the Boltzmann principle in the analysis of the phase stability of $CH_3NH_3Pb(I_{1-x}Br_x)_3$. Their numerical results suggest that the energy of mixing of MAPbI₃ and MAPbBr₃ deviates slightly from that for regular solution. However, they did not discuss the effect of the size difference between Br and I ions. According to the work by Shannon [22], the ionic radii of Br and I ions are 0.196 and 0.221 nm, respectively. There is 12.8% in the size difference, which can introduce local strain and influence the phase separation of mixed halide perovskites.

The migration of ions in halide perovskites can also have positive effects on the performance of some perovskite-based devices under light irradiation [23, 24]. For example, resistance-based memory devices [25, 26] and photodetectors [27, 28] utilizing the phenomenon of the migration of ions in perovskites have been demonstrated. Realizing the effects of the phase separation on the optoelectronic performance of the devices and systems made from mixed-halide perovskites and the possible contribution of local strain from the size mismatch between halide ions to the phase separation, we include the contribution of local strain energy from the size mismatch between halide ions in Gibbs free energy and determine the condition for the presence of phase separation/segradation in mixed halide perovskites under the framework of thermodynamics. The possible migration of halide ions from a halide-perovskite film to a polymer film is also discussed to mimic the scenario of a halide-perovskite film in direct contact with a polymer-based carrier film.

Thermodynamic analysis

Consider a mixed-halide perovskite film $(ABX_xY_y \text{ with } x+y=3)$. Here, A=MA $(CH_3NH_3^+)$, FA $(HC(NH_2)_2^+)$ or Cs, B=Pb or Sn, and X, Y = Cl, Br and I. The mixed halide perovskite is assumed to be formed from the reaction between ABX_3 and ABY_3 . Figure 1(a) shows an example of the formation of $CsPbI_2Br$ with its crystal structure from the CIF file (ID: 8000558) of Crystallography Open Database and the references of [29, 30]. Equation (1) illustrates the corresponding chemical reaction,

$$\frac{x}{3}ABX_3 + \frac{y}{3}ABY_3 \to ABX_xY_y + \Delta H \tag{1}$$

Here, ΔH is the enthalpy of formation for the chemical reaction of (1) and can be calculated as

$$\Delta H = \Delta_{\rm f} H({\rm ABX}_x {\rm Y}_y) - \frac{x}{3} \Delta_{\rm f} H({\rm ABX}_3) - \frac{y}{3} \Delta_{\rm f} H({\rm ABY}_3)$$
 (2)

with $\Delta_f(\cdot)$ representing the standard enthalpy of formation of the corresponding chemical compound. Note that ABX_xY_y can be treated as a binary solution of ABX_3 and ABY_3 with X occupying Y sites in ABY_3 and vice versa. Thus, we can approximate ABX_xY_y as X_xY_y with As and Bs remaining unchanged and X_xY_y as a binary solution of X and Y, as shown in figure 1(b).

According to the theory of thermodynamics [31], the enthalpy of formation, ΔH , for the formation of a binary solution of ABX_xY_y can be thus calculated as

$$\Delta H = P_{XY}\varepsilon = P_{XY} \left[\varepsilon_{XY} - \frac{1}{2} (\varepsilon_{XX} + \varepsilon_{YY}) \right]$$
 (3)

with $\varepsilon_{IJ}(I, J = X \text{ and/or } Y)$ representing the bonding energy between I atom (ion) and J atom (ion), and P_{XY} as the number of bonds between X and Y. For one mole of ABX_xY_y in the form of regular solution with N_X atoms of X from the ABX_3 and N_Y atoms of Y from the $ABY_3(N_X + N_Y = 3N_a \text{ with } N_a \text{ as the Avogadro constant})$, the enthalpy of formation for the formation of a regular, binary solution of ABX_xY_y is [31]

$$\Delta H = \Omega \frac{N_X N_Y}{N_X + N_Y} \text{ and } \Omega = z\varepsilon$$
 (4)

with z as the coordination number of halide atoms/ions in the structure. For ε less than zero, the reaction is exothermic; for ε larger than zero, the reaction is endothermic.

For one mole of ABX_xY_y with N_X number of X and N_Y number of Y, the total configuration states, ω , are

$$\varpi = \frac{(N_X + N_Y)!}{(N_X)!(N_Y)!}$$
 (5)

Thus, the entropy of mixing for the mixing of ABX₃ monomers and ABY₃ monomers is

$$S_{\text{mix}} = k \ln \varpi = -k \left(N_X \ln \frac{N_X}{N_X + N_Y} + N_Y \ln \frac{N_Y}{N_X + N_Y} \right)$$
 (6)

which gives the entropy change from the mixing as

$$\Delta S = -k \left(N_X \ln \frac{N_X}{N_X + N_Y} + N_Y \ln \frac{N_Y}{N_X + N_Y} \right) \tag{7}$$

Here, k is the Boltzmann constant. Note that equation (6) is based on negligible change in vibrational entropy. It is known that there exists the effect of atomic size on the solubility of a binary system, as revealed by the Hume-Rothery rule [32]. The difference in the ionic sizes between X and Y, such as bromine and iodine ions, can introduce local strain through local contraction or expansion, which likely contributes to the enthalpy of formation for the ABX_xY_y and influences the diffusion of X and Y. Wert and Zener [33] discussed the contribution of local strain energy from interstitial solute atoms to the potential energy for the migration of the interstitial solute atoms and incorporated the contribution of local strain energy in the pre-factor of the diffusion coefficient in the analysis of interatomic diffusion. The theoretical result was supported by the experimental results of C in γ -Fe and C, N, and O in tantalum. Zener [34] discussed the effect of local strain energy from the size difference between solute atoms and solvent atoms on elastic modulus of crystalline materials. Machlin [35] and Orian [36] discussed the roles of the strain energy due to an off-size solute atom in the thermodynamics of solid solution. Li et al [37] pointed out that both the partial molar strain energy and the total work done to add a solute atom need to be included in the calculation of the chemical potential of the mobile component for a stressed solid. Recently, Myhill [38] suggested that 'In very dilute solid solutions, elastic strain energies are local' and 'the proportion of each endmember is sufficiently large that the exchanging atoms have overlapping strain fields' in forming a solid solution. It is worth noting that the solid solution strengthening in crystalline metals is based on the interaction between local strain field around solute atoms and dislocations. However, the local strain from the size mismatch of atoms is inaccessible [39] because this is an intrinsic characteristic of a solid solution and the solid solution is at a self-equilibrium state without external stimulus. Also, a uniform strain can be produced in a solid solution with a uniform distribution of solute atoms, while there exists a change in the interaction between atoms.

Let the molal volumes of X and Y be V_X and V_Y , respectively. Thus, the volume of X_XY_Y , V, in the ABX $_XY_Y$ can be approximately calculated as

$$V = xV_X + yV_Y \tag{8}$$

Note that equation (8) is rigorous if both the V_X and V_Y are the corresponding partial molal volumes. In general, one can approximate the corresponding partial molal volumes to be V_X and V_Y . Using the molal volumes of V_X and V_Y , we have atomic/ionic volumes of V_X/N_a and V_Y/N_a for the X atoms/ions and the Y atoms/ions, respectively.

Consider one mole of ABX_xY_y, which is formed with the reaction of (1). There are N_X atoms/ions of X and N_Y atoms/ions of Y from the ABX₃ and the ABY₃, respectively. Local strain is introduced if an ion of X of V_X/N_a in ionic volume is replaced by an ion of Y of V_Y/N_a in ionic volume and vice versa. For $V_X > V_Y$, the Y ions in the ABX₃ experience tension; for $V_X < V_Y$, the Y ions in the ABX₃ experience compression. A similar deformation state applies to the X ions in the ABY₃. The difference in the ionic volumes introduces volumetric strains as ω_{ABX_3}/N_a for an ion of X in a unit cell of ABX₃ being replaced by an ion of Y in ABY₃ and ω_{ABY_3}/N_a for an ion of Y in a unit cell of ABY₃ being replaced by an ion of X in ABX₃. Here, ω_{ABX_3} and ω_{ABY_3} are the molar volume expansion coefficients of the ABX₃ and ABY₃, respectively, which is due to the ionic replacement and proportional to $(V_Y - V_X)/V_X$ and $(V_X - V_Y)/V_Y$, respectively.

For the formation of one mole ABX_xY_y from the ABX_3 and ABY_3 , let us first consider the condition of N_X being smaller than N_Y . Assume that the formation of ABX_xY_y leads to the exchange of αN_X ions of X in the ABX_3 with αN_X ions of Y in the ABY_3 for α less than or equal to 1. According to equations (A5)–(A6) in appendix, the strain energy in one mole of ABX_xY_y due to the size mismatch can be approximately calculated as

$$E = \frac{1}{3} \frac{N_X}{N_a} V_X E_{X \to Y} + \frac{1}{3} \frac{N_Y}{N_a} V_Y E_{Y \to X} = \frac{1}{6} \alpha^2 \left(V_X K_X \omega_{ABX_3}^2 \frac{N_X}{N_a} + V_Y K_Y \omega_{ABY_3}^2 \frac{N_Y}{N_a} \right) \left(\frac{N_X}{N_a} \right)^2$$
(9)

Using equations (4), (7) and (9), we obtain the change of the Gibbs free energy for the formation of one mole of ABX_xY_y from the ABX_3 and ABY_3 as

$$\Delta G = \Delta H - T\Delta S + E
= \Omega \frac{N_X N_Y}{N_X + N_Y} + kT \left(N_X \ln \frac{N_X}{N_X + N_Y} + N_Y \ln \frac{N_Y}{N_X + N_Y} \right)
+ \frac{1}{6} \alpha^2 \left(V_X K_X \omega_{ABX_3}^2 \frac{N_X}{N_a} + V_Y K_Y \omega_{ABY_3}^2 \frac{N_Y}{N_a} \right) \left(\frac{N_X}{N_a} \right)^2$$
(10)

To have a stable single phase of ABX_xY_y , it requires the Gibb free energy to be minimum at the composition of N_X and N_Y under constant pressure and temperature, i.e.,

$$\frac{\partial \Delta G}{\partial N_X} = \frac{\partial \Delta G}{\partial N_Y} = 0 \text{ and } \frac{\partial^2 \Delta G}{\partial N_X^2} \cdot \frac{\partial^2 \Delta G}{\partial N_Y^2} - \left(\frac{\partial^2 \Delta G}{\partial N_X \partial N_Y}\right)^2 > 0 \text{ with } \frac{\partial^2 \Delta G}{\partial N_X^2} > 0$$
 (11)

With the presence of the stable single phase of ABX_xY_y , a mixture of ABX_xY_y and ABX_3 or ABX_xY_y and ABY_3 can be formed likely with local segregation of ABX_3 or ABY_3 . This is associated with the phase instability of mixed halide perovskites.

Taking partial derivatives with respect to N_X and N_Y , respectively, we obtain the chemical potentials as

$$\mu_{ABX_3} = \mu_{ABX_3}^0 + \Omega \left(\frac{N_Y}{N_X + N_Y}\right)^2 + kT \ln \frac{N_X}{N_X + N_Y} + \frac{1}{3}\alpha^2 \left(\frac{3}{2}V_X K_X \omega_{ABX_3}^2 \frac{1}{N_a} + V_Y K_Y \omega_{ABY_3}^2 \frac{N_Y}{N_X N_a}\right) \left(\frac{N_X}{N_a}\right)^2$$
(12)

for one X in the ABX, Y, and

$$\mu_{ABY_3} = \mu_{ABY_3}^0 + \Omega \left(\frac{N_X}{N_X + N_Y} \right)^2 + kT \ln \frac{N_Y}{N_X + N_Y} + \frac{1}{6} \alpha^2 V_Y K_Y \omega_{ABY_3}^2 \frac{1}{N_a} \left(\frac{N_X}{N_a} \right)^2$$
(13)

for one Y in the ABX_xY_v .

Under the condition of N_X being larger than N_Y , we assume that the formation of ABX_xY_y leads to the exchange of βN_Y ions of Y in the ABY_3 with βN_Y ions of X in the ABX_3 for β less than or equal to 1. Following similar approach to the case with N_X being smaller than N_Y , we obtain the change of the Gibbs free energy for the formation of one mole of ABX_xY_y , as given in equation (A8) in appendix. Using equation (A8), the chemical potentials are found as

$$\mu_{ABX_3} = \mu_{ABX_3}^0 + \Omega \left(\frac{N_Y}{N_x + N_Y}\right)^2 + kT \ln \frac{N_X}{N_X + N_Y} + \frac{1}{6} \beta^2 V_X K_X \omega_{ABX_3}^2 \frac{1}{N_a} \left(\frac{N_Y}{N_a}\right)^2$$
(14)

for one X in the ABX_xY_y , and

$$\mu_{ABY_3} = \mu_{ABY_3}^0 + \Omega \left(\frac{N_X}{N_X + N_Y} \right)^2 + kT \ln \frac{N_Y}{N_X + N_Y} + \frac{1}{3} \beta^2 \left(V_X K_X \omega_{ABX_3}^2 \frac{N_X}{N_Y N_a} + \frac{3}{2} V_Y K_Y \omega_{ABY_3}^2 \frac{1}{N_a} \right) \left(\frac{N_Y}{N_a} \right)^2$$
(15)

for one Y in the ABX_xY_y .

According to equation (1), there are

$$N_X = xN_a \text{ and } N_Y = yN_a$$
 (16)

for one mole of ABX_xY_y. Using equation (16) and x + y = 3, equations (12)–(15) are rewritten as

$$\mu_{ABX_3} = \mu_{ABX_3}^0 + \Omega \left(\frac{3-x}{3}\right)^2 + kT \ln \frac{x}{3} + \frac{1}{3}\alpha^2 \left(\frac{3}{2}V_X K_X \omega_{ABX_3}^2 + V_Y K_Y \omega_{ABY_3}^2 \frac{3-x}{x}\right) \frac{x^2}{N_a}$$
(17)

$$\mu_{ABY_3} = \mu_{ABY_3}^0 + \Omega \left(\frac{3-y}{3}\right)^2 + kT \ln \frac{y}{3} + \frac{1}{6}\alpha^2 V_Y K_Y \omega_{ABY_3}^2 \frac{(3-y)^2}{N_a}$$
 (18)

for x less than y in the ABX_xY_y, and

$$\mu_{ABX_3} = \mu_{ABX_3}^0 + \Omega \left(\frac{3-x}{3}\right)^2 + kT \ln \frac{x}{3} + \frac{1}{6}\beta^2 V_X K_X \omega_{ABX_3}^2 \frac{(3-x)^2}{N_a}$$
 (19)

$$\mu_{ABY_3} = \mu_{ABY_3}^0 + \Omega \left(\frac{3-y}{3}\right)^2 + kT \ln \frac{y}{3} + \frac{1}{3}\beta^2 \left(V_X K_X \omega_{ABX_3}^2 \frac{3-y}{y} + \frac{3}{2} V_Y K_Y \omega_{ABY_3}^2\right) \frac{y^2}{N_a}$$
(20)

for x larger than y in the ABX_xY_y .

According to the theory of thermodynamics [31], the two phases at equilibrium satisfy the following conditions

$$\mu_{ABX_2}(x_1/3) = \mu_{ABX_2}(x_2/3) \tag{21}$$

$$\mu_{ABY_2}(1 - x_1/3) = \mu_{ABY_2}(1 - x_2/3) \tag{22}$$

The solutions of equations (21)–(22) determine the compositions of the phases (x_1 and x_2) at equilibrium in the mixed form of ABX_xY_y at temperature T. It should be noted that numerical calculation is needed to solve the set of equations (21)–(22).

The critical point for phase separation, if exists, is determined by the following two equations

$$\frac{\partial^2 \Delta G}{\partial x^2} = 0 \text{ and } \frac{\partial^3 \Delta G}{\partial x^3} = 0$$
 (23)

which give

$$\frac{kT}{x}\left(1 + \frac{x}{3-x}\right) + \frac{\alpha^2}{N_a}[V_X K_X \omega_{ABX_3}^2 x - V_Y K_Y \omega_{ABY_3}^2 (x-1)] = \frac{2}{3}\Omega$$
 (24)

$$-\frac{kT}{x^2} + \frac{kT}{(x-3)^2} + \frac{\alpha^2}{N_a} [V_X K_X \omega_{ABX_3}^2 - V_Y K_Y \omega_{ABY_3}^2] = 0$$
 (25)

for x less than y in the ABX_xY_y, and

$$\frac{kT}{x}\left(1+\frac{x}{3-x}\right)+\frac{\beta^2}{N_a}[V_XK_X\omega_{ABX_3}^2(x-2)-V_YK_Y\omega_{ABY_3}^2(x-3)]=\frac{2}{3}\Omega$$
 (26)

$$-\frac{kT}{x^2} + \frac{kT}{(x-3)^2} + \frac{\beta^2}{N_c} [V_X K_X \omega_{ABX_3}^2 - V_Y K_Y \omega_{ABY_3}^2] = 0$$
 (27)

for x larger than y in the ABX_xY_y .

The above analysis is focused on the formation of the ABX_xY_y from the ABX_3 and ABY_3 . It is known that the perovskite film/layer in a perovskite-based photovoltaic cell is sandwiched between electron and hole transfer layers/films. There have been great works of using organic carrier transfer layers (polymer-based layers) in perovskite-based photovoltaic cells due to unique characteristics of organic carrier transfer layers, including tunable bandgap, facile solution-based synthesis, and low cost [40]. However, the direct contact between an organic carrier transfer layer and a perovskite layer allows for atomic migration, such as halogen atoms (Cl, Br and I), across the interface between the organic carrier transfer layer and the perovskite layer due to the difference of Gibbs free energies, leading to the structural changes of the perovskite layer.

According to the results reported by Li *et al* [41], iodine in APbI₃ (A = Cs or MA) migrates across the interface between the APbI₃ film and the [6,6]-phenyl-C61-butyric acid methyl ester, leading to the performance changes of associated photovoltaic cells. The driving force for the migration of iodine is the difference of the chemical potentials of iodine. If the contribution of the strain energy associated with the migration of iodine to the chemical potential of iodine is negligible, the driving force for the migration of iodine is the difference of the iodine concentrations between the APbI₃ film and the [6,6]-phenyl-C61-butyric acid methyl ester.

Consider the contact between an ABX₃ film and a polymer film (carrier transfer layer), mimicking the bilayer structure used in photovoltaic cells made from halide perovskites. The contact between the ABX₃ and the polymer film introduces the concentration difference of A, B and X between the ABX₃ film and the polymer film, respectively. Interdiffusion can occur between the ABX₃ film and the polymer film, in which the diffusion (migration) rates of elements and polymer chains are dependent on the bonding strength of the elements to the ABX₃ film and the cohesive strength of polymer chains in the polymer film.

The diffusion of X element from the ABX₃ film to the polymer film leaves anion vacancies in the ABX₃ film. The difference in the linear dimension of an anion vacancy and the size of X ion in the ABX₃ film introduces local strains at anion vacancies. Let ω_{\square} be the molar volume expansion coefficient for the replacement of X ions by anion vacancies in the ABX₃ film. The associated strain energy density is

$$E_{\square} = \frac{1}{2} K_X x_{\square}^2 \omega_{\square}^2 \tag{28}$$

with x_{\square} as the molar fraction of anion vacancies replacing the X ions in the ABX₃ film. Accordingly, the strain energy in χ mole of ABX₃ due to the size mismatch between the anion vacancy and X anion can be approximately calculated as

$$E_T = \frac{1}{2} \chi K_X x_{\square}^3 \omega_{\square}^2 \tag{29}$$

The change of the Gibbs free energy of χ mole of ABX₃ (the ABX₃ film) due to the migration of X ions to the polymer film is

$$\Delta G_T = \Delta H_T - T \Delta S_T + E_T \tag{30}$$

Here, the enthalpy of formation of anion vacancies, ΔH_T , is

$$\Delta H_T = \chi x_{\square} \Delta H_{\square} \tag{31}$$

and ΔS_T is

$$\Delta S_T = \chi R \left[x_{\square} \ln \frac{x_{\square}}{3} + (3 - x_{\square}) \ln \frac{3 - x_{\square}}{3} \right]$$
 (32)

which gives

$$\Delta G_T = \chi x_{\square} \Delta H_{\square} - \chi RT \left[x_{\square} \ln \frac{x_{\square}}{3} + 3 \ln \frac{3 - x_{\square}}{3} \right] + \frac{1}{2} \chi K_X x_{\square}^3 \omega_{\square}^2$$
 (33)

Thus, the chemical potential of X ions in the ABX3 film is

$$\mu_X = \frac{\partial \Delta G_T}{\partial x_{\square}} = \chi \Delta H_{\square} - \chi RT \ln \frac{x_{\square}}{3 - x_{\square}} + \frac{3}{2} \chi K_X x_{\square}^2 \omega_{\square}^2$$
 (34)

Assume that there are m_p mole sites available to host x_{\square} number of X atoms in the polymer film and the mechanical deformation of the polymer film due to the presence of X atoms is negligible. For a dilute solution of X atoms in the polymer film, the chemical potential of X atoms in the polymer film is

$$\mu_p = m_p RT \ln \frac{x_{\square}}{m_p} \tag{35}$$

At equilibrium, there is

$$m_p RT \ln \frac{x_{\square}}{m_p} = \chi \Delta H_{\square} - \chi RT \ln \frac{x_{\square}}{3 - x_{\square}} + \frac{3}{2} \chi K_X x_{\square}^2 \omega_{\square}^2$$
 (36)

which determines the number of X atoms diffusing into the polymer film and the corresponding defects (anion vacancies) presented in the ABX $_3$ film. The diffusion of the X atoms in the ABX $_3$ film to the polymer film causes the deterioration of the ABX $_3$ film and the degradation of the optoelectronic characteristics of the structure with the ABX $_3$ film.

It should be noted that the above analysis is focused on the system consisting of two 'mobile' components (X and Y or X and anion vacancy). Such an approach can be extended to multiple 'mobile' components in mixed cation perovskites and mixed-cation mixed-halide perovskites, if the information for the exchanges of ions/ atoms is available. However, the Gibb free energy of such a system is likely much more complex than the system studied in this work, and more tedious analysis is needed to illustrate the dependence of the Gibb free energy on the chemical compositions of mixed-cation mixed-halide perovskites and the composition dependence of the phase stability of mixed-cation mixed-halide perovskites.

Numerical calculation

Here, the phase stability of the MAPbI_xBr_{3-x} mixed halide perovskite is numerically analyzed. Using the quasichemical approximation method [42], Brivio *et al* [21] obtained the numerical value of Ω to be 0.06-0.02(1-x/3) eV/anion. The ionic radii of Br⁻ and I⁻ are 0.196 and 0.221 nm, respectively; the bulk moduli of MAPbBr₃ and MAPbI₃ are 15.9 and 15.6 GPa [43], respectively. Accordingly, there are

$$V_{I^{-}} = \frac{4\pi}{3} N_a r_{I^{-}}^3 = 2.72 \times 10^{-5} \text{m}^3 \text{ and } V_{Br^{-}} = \frac{4\pi}{3} N_a r_{Br^{-}}^3 = 1.90 \times 10^{-5} \text{m}^3$$
 (37)

IOP Publishing Phys. Scr. 99 (2024) 025937 F Yang

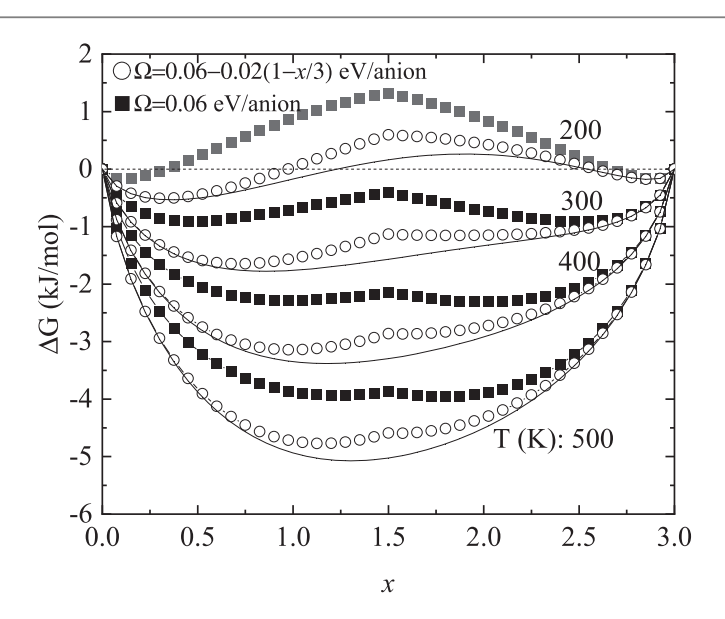


Figure 2. Variation of the change of the Gibbs free energy with x for $\lambda = 0.1$ at different temperatures of 200, 300, 400 and 500 K. The solid lines represent the results with $\Omega = 0.06 - 0.02(1 - x/3)$ eV/anion and $\Im(x) = 0$; the open circle symbols represent the results with $\Omega = 0.06 - 0.02(1 - x/3)$ eV/anion and the contribution of the strain energy; and the solid square symbols represent the results with $\Omega = 0.06 \, \mathrm{eV/anion}$ and the contribution of the strain energy.

Using equation (13), we have

$$\omega_{\text{MAPbI}_3} = \lambda_1 \frac{V_{Br^-} - V_{I^-}}{V_{I^-}} = -0.302\lambda_1 \text{ and } \omega_{\text{MAPbBr}_3} = \lambda_2 \frac{V_{I^-} - V_{Br^-}}{V_{Br^-}} = 0.434\lambda_2$$
 (38)

with λ_1 and λ_2 being proportionality constants. It is evident that there are more than 30% volumetric strains induced by the replacement of I-ions by Br-ions and vice versa, if $\lambda_1 \approx \lambda_2 \approx 1$. Note that $\lambda_1 = \lambda_2 = 1$ for dilute solid solutions. For non- dilute solid solutions, numerical calculation, such as finite element method, is needed to determine the variation of both λ_1 and λ_2 with the fraction of solute atoms in a solid solution.

Using the above numerical data, the change of the Gibbs free energy in the unit of J/mol for the formation of the MAPbI_xBr_{3-x} mixed halide perovskite from MAPbI₃ and MAPbBr₃ is

$$\Delta G = 96485[0.06 - 0.02(1 - x/3)] \frac{x(3 - x)}{3} + 8.313T \left[x \ln \frac{x}{3} + (3 - x) \ln \frac{3 - x}{3} \right] + \mathcal{I}(x)$$
 (39)

The function $\Im(x)$ is defined as

$$\mathcal{I}(x) = \frac{1}{6} \begin{cases} \alpha^2 (3.87\lambda_1^2 x + 5.69\lambda_2^2 (3 - x))x^2 \times 10^4 & \text{for } x \text{ less than } 1.5\\ \beta^2 [3.87\lambda_1^2 x + 5.69\lambda_2^2 (3 - x)](3 - x)^2 \times 10^4 & \text{for } x \text{ larger than } 1.5 \end{cases}$$
(40)

For simplification, we let $\alpha = \beta = 0.9$ and $\lambda_1 = \lambda_2 = \lambda$. Figure 2 shows the variation of the change of the Gibbs free energy with x for $\lambda = 0.1$ at different temperatures. For comparison, the results with $\Im(x) = 0$ are also included in figure 2, in which the solid lines represent the results without the contribution of the strain energy and the open circle symbols represent the results with the contribution of the strain energy. In general, the change of the Gibbs free energy with the contribution of the strain energy exhibits similar trend to that without the contribution of the strain energy. For example, there exists a range of x, in which the change of the Gibbs free energy is positive for both conditions and MAPbI_xBr_{3-x} mixed halide perovskite cannot be formed. However, the magnitude of the negative change of the Gibbs free energy with the contribution of the strain energy is generally smaller than the corresponding one without the contribution of the strain energy under the same condition, which indicates that the strain energy from the size match between I and Br ions reduces the energy barrier for the onset of phase separation. The strain energy widens the x range with positive change of the Gibbs free energy, i.e., the range without the presence of the mixed halide perovskite. Such a result suggests that the strain energy due to the size mismatch of halide ions likely increases the structural instability of mixed halide perovskites, and the size mismatch of halide ions reduces the resistance to the phase separation of a mixed halide perovskite. Also, two structures can coexist—one with Br⁻ as the solute ion and the other with I as the solute ion. It should be pointed out that the numerical calculation is based on that the parameters of α , β , λ_1 and λ_2 are constants, independent of x (the molar/volumetric fractions of individual MAPbBr₃ and MAPbI₃). These parameters may be functions of the molar/volumetric fractions of individual phases (MAPbBr₃ and MAPbI₃).

The first principles calculation is needed to investigate the possible dependence of these parameters on the molar/volumetric fractions of individual phases (MAPbB $_{13}$).

It needs to be pointed out that Brivio $et\,al\,[21]$ did not provide the information of the parameters used in the calculation of Ω , and it is unclear if they included the contribution of the strain energy from the size mismatch in the calculation of Ω . We then use $\Omega=0.06$ in the numerical calculation, which corresponds to the regular solution, and includes the results in figure 2, as represented by the solid square symbols, for the purpose of comparison. For the case with $\Omega=0.06\,{\rm eV/anion}$ and the contribution of the strain energy, the change of the Gibbs free energy with x exhibits similar trend to the other cases with $\Omega=0.06-0.02(1-x/3)\,{\rm eV/anion}$. However, the numerical result of the change of the Gibbs free energy is much larger than the corresponding ones with $\Omega=0.06-0.02(1-x/3)\,{\rm eV/anion}$ with and without the contribution of the strain energy. Such a large difference reveals the effect of the term of -0.02(1-x/3) and likely suggests that the formulation of $\Omega=0.06-0.02(1-x/3)\,{\rm eV/anion}$ might not include the contribution of the strain energy from the size mismatch.

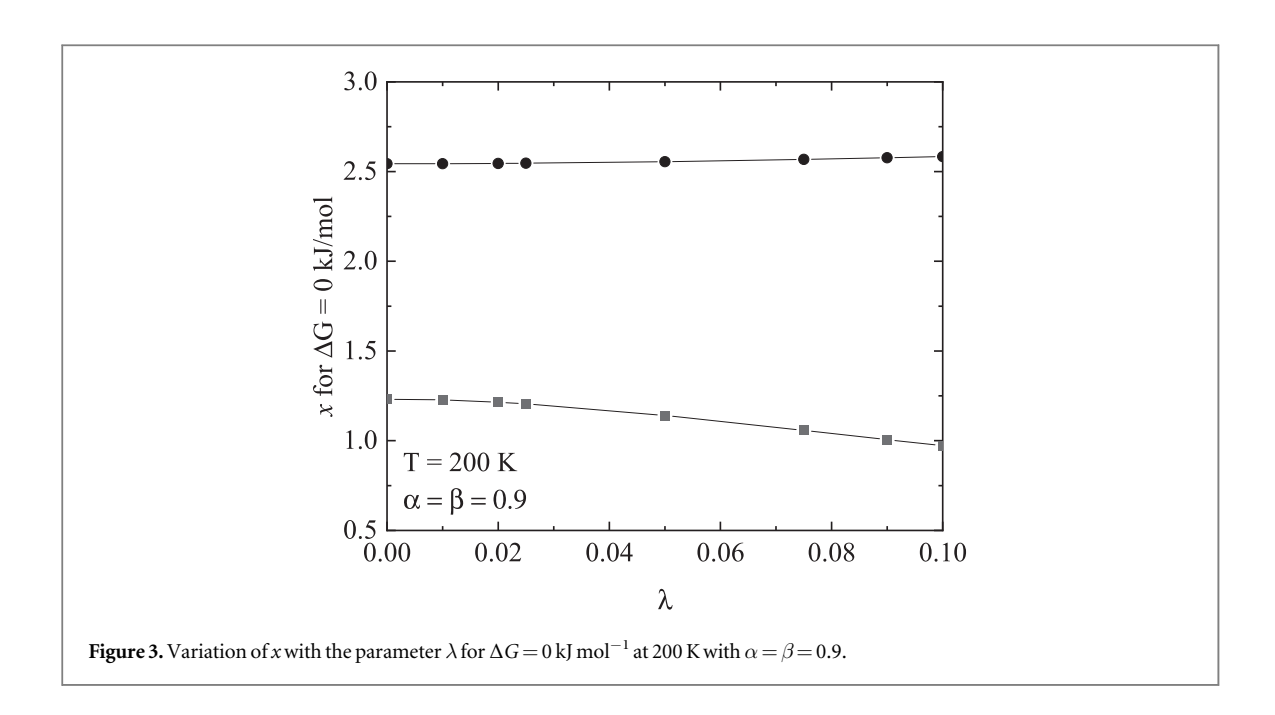
According to equation (11), there are two stable compositions for MAPbI $_x$ Br $_{3-x}$ mixed halide perovskites at 200 K for the cases with $\Omega=0.06-0.02(1-x/3)$ eV/anion and the contribution of the strain energy and with $\Omega=0.06-0.02(1-x/3)$ eV/anion and $\Im(x)=0$, at which the change of Gibbs free energy reaches local minimum. One can be considered as a substitutional solid solution of MAPbBr $_3$ with added I for small x, and the other as a substitutional solid solution of MAPbI $_3$ with added Br for large x. The corresponding compositions are (MAPbI $_{0.34}$ Br $_{2.66}$, MAPbI $_{2.89}$ Br $_{0.11}$) and (MAPbI $_{0.36}$ Br $_{2.64}$, MAPbI $_{2.89}$ Br $_{0.11}$) for the cases with $\Omega=0.06-0.02(1-x/3)$ eV/anion and the contribution of the strain energy and with $\Omega=0.06-0.02(1-x/3)$ eV/anion and $\Im(x)=0$, respectively. Including the contribution of the strain energy from the size mismatch between Br $^-$ and I $^-$ ions in the change of Gibbs free energy leads to a slight decrease of x from 0.36 to 0.34, i.e., the chemical composition of the stable substitutional solid solution of MAPbBr $_3$ changes from MAPbI $_{0.36}$ Br $_{2.64}$ to MAPbI $_{0.34}$ Br $_{2.66}$ with the contribution of the strain energy. Note that there is almost no change to the chemical composition of the stable substitutional solid solution of MAPbI $_3$ with added Br.

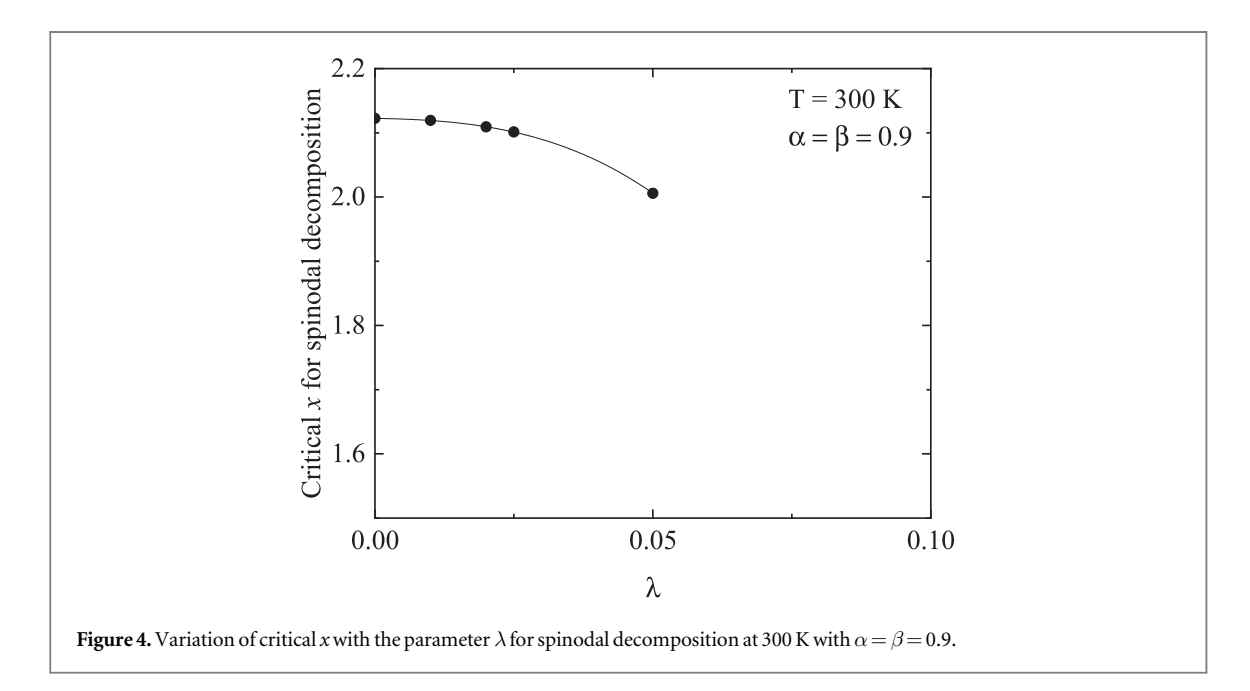
There likely exist a region of x for MAPbI $_x$ Br $_{3-x}$ mixed halide perovskites for temperature in the range of 300 and 500 K for the case with $\Omega=0.06-0.02(1-x/3)$ eV/anion and the contribution of the strain energy, in which MAPbI $_x$ Br $_{3-x}$ mixed halide perovskites are unstable. For a MAPbI $_x$ Br $_{3-x}$ mixed halide perovskite with x failing in this region, any small perturbation to the system and/or the nucleation of the stable solid solutions can lead to phase separation/degradation of the MAPbI $_x$ Br $_{3-x}$ mixed halide perovskite to two co-existing substitutional solid solutions, as determined by the common tangent, in consistence with the observations reported in the literature [44, 45]. For the case with $\Omega=0.06$ -0.02(1-x/3) eV/anion and $\Im(x)=0$, no binodal region is present for temperature larger than or equal to 300 K. Any MAPbI $_x$ Br $_{3-x}$ mixed halide perovskite with $\partial \Delta G/\partial x \neq 0$ is metastable. It requires the nucleation of new structures with the composition corresponding to $\partial \Delta G/\partial x = 0$ for the onset of the phase separation.

According to equation (39), the strain energy from the size match between Γ and Γ ions is equal to the difference between the changes of Gibbs free energy with $\Omega=0.06-0.02(1-x/3)$ eV/anion and the contribution of the strain energy and with $\Omega=0.06-0.02(1-x/3)$ eV/anion and $\Im(x)=0$. Thus, the difference between the changes of Gibbs free energy with $\Omega=0.06-0.02(1-x/3)$ eV/anion and the contribution of the strain energy and with $\Omega=0.06-0.02(1-x/3)$ eV/anion and $\Im(x)=0$ shown in figure 2 at different temperatures provides the information on the variation of the strain energy from the size match between Γ and Π ions with Π .

Figure 3 presents the variations of the lower and upper bounds of x with the parameter λ at 200 K, in which no MAPbI $_x$ Br $_{3-x}$ mixed halide perovskite can be formed. Increasing λ leads to the decrease of the lower bound of x and a slight increase of the upper bound of x. That is to say, increasing the mismatch strain widens the range of x, in which no MAPbI $_x$ Br $_{3-x}$ mixed halide perovskite can be formed, i.e., increasing the mismatch strain increases the range of x for the phase instability of MAPbI $_x$ Br $_{3-x}$ mixed halide perovskite. Such a result is qualitatively in accord with the observation by Ni *et al* [46] in the study of the Br effect on the phase stability of H $_2$ N=CHNH $_2$ Pb(I $_{1-x}$ Br $_x$) $_3$ films. They found that increasing the fraction of Br caused the increase in lattice constant (volume expansion) and the decrease of the phase stability of H $_2$ N=CHNH $_2$ Pb(I $_{1-x}$ Br $_x$) $_3$ films for x larger than 0.05.

Figure 4 presents the variation of critical x for spinodal decomposition with the parameter λ at 300 K and $\alpha = \beta = 0.9$, which is determined by the conditions of (24) and (26). It is interesting to note that the critical value of x decreases with the increase of λ (mismatch strain) for x larger than y. Such a result suggests that λ is likely a function of x, which requires the first principles calculation to determine the correlation between λ and x. Note that there is no solution for x less than 1.5 (y), i.e., no spinodal decomposition can take place for the substitutional solid solution of MAPbBr₃ with added I for constant λ . Such a result suggests that it requires the nucleation of new structures of the stable substitutional solid solution for the onset of the phase separation. It also should be pointed out that no real solution of x can be obtained in the range of 1.5 to 3 for λ larger than 0.056.





Discussion

The analysis presented in this work is solely based on the size mismatch between halide ions in the framework of linear elasticity of isotropic and homogeneous materials. The crystal structure of halide perovskites is much more complicated, and the use of isotropic and homogeneous characteristics for mixed halide perovskites in the analysis is a first-order approximation without considering the contributions of nearby structures (ionic arrangements) to local deformation and strain energy. Also, this study only considers the contribution of configurational entropy to the Gibb free energy. It is unclear if vibrational entropy plays a role in the phase stability of halide perovskites and mixed halide perovskites. Further analysis of the effects of nearby structures (ionic arrangements) on the local deformation and strain energy and the contribution of vibrational entropy with molecular mechanics and statistic thermodynamics is likely to reveal the dependence of the phase stability and transition of mixed halide perovskites on ionic arrangements and vibrational entropy.

The numerical results reveal the effects of mechanical strain due to the size mismatch on the phase stability of $MAPbI_xBr_{3-x}$ mixed halide perovskite and the critical molar fractions of I ions (MAPbI₃) for spinodal decomposition. Such results are based on the theory of equilibrium thermodynamics, which cannot predict and assess the migration/diffusion of ions/atoms associated with the evolution of the phase stability. To understand

the process controlling the evolution of the phase stability, it requires the analysis of the migration/diffusion of halide ions.

It is known that the driving force for the migration/diffusion of mobile components is the gradient of chemical potential of the mobile components. If there are no contributions of external fields to the chemical potential of the mobile components, the driving force is the gradient of the concentration of the mobile components. Under the action of mechanical stress, including self-stress, the chemical potential of the mobile components is dependent on local stress/strain, as revealed in equations (17)–(20). The spatial distribution of local stress/strain will introduce non-zero gradient of the stress/strain, which limits the migration/diffusion of the mobile components.

Also, the migration/diffusion of mobile components is a thermally activated process. The diffusion coefficient of the mobile components, D, as a function of temperature can be expressed by an Arrhenius-like equation as

$$D = D_0 \exp(-Q/RT) \tag{41}$$

with D_0 as a pre-exponential factor, and Q is the activation energy. In general, the activation energy for the motion of ions/atoms at the stress-free state is the difference of the potential energies between the activated state (the saddle point) and the equilibrium state [47], which depends on the interaction between the ions/atoms and adjacent ions/atoms. This interaction significantly depends on the structure of crystals. The loose structure of halide perovskites leads to a weak interaction between an ion/atom and adjacent ions/atoms, which has small resistance and small energy barrier (activation energy) to the motion of the ion/atom. The ion/atom thus has a large probability to migrate under a small driving force (the gradient of chemical potential) in mixed halide perovskites, resulting in phase separation (phase stability). To mitigate the phase instability associated with the strain energy from intrinsic size mismatch and/or light-induced expansion, strain and/or field engineering, such as high pressure, can be likely applied to introduce strain and/or field gradient to increase the energy barrier for the motion of halide ions and counterbalance the gradient of chemical potential, including the strain gradient by the mismatch strain and/or light-induced expansion.

Under the action of mechanical stress/strain, including self-stress, the activation energy becomes dependent on local stress and can be expressed as

$$Q = Q_0 + \Delta Q \tag{42}$$

where Q_0 is the activation energy without mechanical stress, and ΔQ represents the deformation-induced change of the activation energy. For non-hydrostatic deformation, ΔQ can be calculated as $P\varpi$ with P as the effective stress and ϖ as the shear activation volume. For hydrostatic deformation, Flynn [48] suggested that ΔQ consists of the contribution from mechanical deformation. All these discussions point to the fact that the diffusion coefficient of mobile components is a function of local stress/strain. Therefore, local stress/strain plays an important role in the migration/diffusion of the mobile species as well as in the phase stability of mixed halide perovskites used in photovoltaic cells.

Summary

In summary, we have brought out the important role of the mismatch strain due to the size difference in the halide ions in the phase stability of mixed halide perovskites. Incorporating the strain energy associated with the mismatch strain in the change of the Gibbs free energy of a mixed halide perovskite formed from the reaction of two different halide perovskites, we have obtained analytical formulas of the chemical potentials of halide ions and established the conditions to determine the lower and upper bounds of the atomic fractions of halide ions for the spinodal decomposition of the mixed halide perovskites.

The direct contact between a perovskite layer and a polymer-based transfer layer in perovskite-based photovoltaic cells can lead to the migration/diffusion of halide ions from the perovskite to the polymer film. Following similar approach to the analysis of the phase stability of mixed halide perovskites, we have also established the condition for the determination of the equilibrium concentration of halogen atoms in the polymer film and revealed the potential role of local stress/strain in the redistribution of halide ions in photovoltaic cells.

Numerical calculations have been performed to analyze the phase stability of $MAPbI_xBr_{3-x}$ mixed halide perovskite. The numerical results show that the strain energy due to the size mismatch causes the decrease in the magnitude of the negative change of the Gibbs free energy and the increase of the range of atomic fraction with the positive change of the Gibbs free energy if it exists.

IOP Publishing *Phys. Scr.* **99** (2024) 025937 FYang

Acknowledgments

This work is supported by the National Science Foundation through the grant CMMI-1854554, monitored by Drs Khershed Cooper and Thomas Francis Kuech, and CBET-2018411 monitored by Dr Nora F Savage.

Data availability statement

All data that support the findings of this study are included within the article (and any supplementary files).

Author contributions

FY contributed to conceptualization, investigation, writing reviewing and editing, project administration, supervision and funding acquisition.

Data and code availability

Not applicable.

Supplementary information

Not applicable.

Declarations

Conflict of interest

There is no conflict of interests to disclose.

Ethical approval

Not applicable.

Appendix

(1) Calculation of strain energy

For the formation of one mole ABX $_x$ Y $_y$ from the ABX $_3$ and ABY $_3$, let us consider the condition of N_X being smaller than N_Y . Assume that the formation of ABX $_x$ Y $_y$ leads to the exchange of αN_X ions of X in the ABX $_3$ with αN_X ions of Y in the ABY $_3$ for α less than or equal to 1. The volumetric strain, $\varepsilon_{X \to Y}$, for αN_X ions of X in the ABX $_3$ being replaced by αN_X ions of Y in the ABY $_3$ can be approximately calculated as

$$\varepsilon_{X \to Y} = \alpha \omega_{ABX_3} \frac{N_X}{N_a} \tag{A1}$$

Similarly, there is

$$\varepsilon_{Y \to X} = \alpha \omega_{ABY_3} \frac{N_X}{N_a} \tag{A2}$$

for αN_X ions of Y in the ABY₃ being replaced by αN_X ions of X in the ABX₃. In the framework of linear

elasticity, the volumetric strains lead to hydrostatic stresses in the ABX₃ and ABY₃, respectively, as

$$\sigma_{X \to Y} = K_X \varepsilon_{X \to Y} = \alpha K_X \omega_{ABX_3} \frac{N_X}{N_c}$$
(A3)

$$\sigma_{Y \to X} = K_Y \varepsilon_{Y \to X} = \alpha K_Y \omega_{ABY_3} \frac{N_X}{N_a}$$
(A4)

with K_X and K_Y as the bulk modulus of the ABX₃ and ABY₃, respectively. Using equations (A1)–(A4), the strain energy densities are calculated to be

$$E_{X \to Y} = \frac{1}{2} \sigma_{X \to Y} \varepsilon_{X \to Y} = \frac{1}{2} K_X \alpha^2 \omega_{ABX_3}^2 \left(\frac{N_X}{N_a} \right)^2$$
 (A5)

for the replacement of αN_X ions of X in the ABX₃ by αN_X ions of Y in the ABY₃, and

$$E_{Y \to X} = \frac{1}{2} K_Y \alpha^2 \omega_{ABY_3}^2 \left(\frac{N_X}{N_a} \right)^2 \tag{A6}$$

for the replacement of αN_X ions of Y in the ABY₃ by αN_X ions of X in the ABX₃.

(2) Gibbs free energy for the formation of one mole of ABX_xY_y from ABX_3 and ABY_3 with N_X larger than N_Y Under the condition of N_X being larger than N_Y , we assume that the formation of ABX_xY_y leads to the exchange of βN_Y ions of Y in the ABY_3 with βN_Y ions of X in the ABX_3 for β less than or equal to 1. Following similar approach to the case with N_X being smaller than N_Y , the strain energy in one mole of ABX_xY_y due to the size mismatch can be approximately calculated as

$$E = \frac{1}{6}\beta^2 \left(V_X K_X \omega_{ABX_3}^2 \frac{N_X}{N_a} + V_Y K_Y \omega_{ABY_3}^2 \frac{N_Y}{N_a} \right) \left(\frac{N_Y}{N_a} \right)^2$$
 (A7)

which yields the change of the Gibbs free energy for the formation of one mole of ABX_xY_y from the ABX_3 and the ABY_3 as

$$\Delta G = \Omega \frac{N_X N_Y}{N_X + N_Y} + kT \left(N_X \ln \frac{N_X}{N_X + N_Y} + N_Y \ln \frac{N_Y}{N_X + N_Y} \right) + \frac{1}{6} \beta^2 \left(V_X K_X \omega_{ABX_3}^2 \frac{N_X}{N_a} + V_Y K_Y \omega_{ABY_3}^2 \frac{N_Y}{N_a} \right) \left(\frac{N_Y}{N_a} \right)^2$$
(A8)

(3) Derivation of the molar volume expansion coefficient

Eshelby [49] discussed the lattice distortion induced by a center of dilatation of strength c in a homogeneous, isotropic elastic material and obtained the change of total volume as

$$\Delta V = \frac{12\pi c(1-\nu)}{1+\nu} \tag{A9}$$

with v as Poisson's ratio of the material. For the center of dilatation being a solute atom of radius r, there is

$$c = \frac{\varepsilon r_0^3 (1+\nu)}{3(1-\nu)} \tag{A10}$$

Here, r_0 is the radius of solvent atom, and $\varepsilon = (r-r_0)/r_0$. Substituting equation (A10) in equation (A9) yields

$$\Delta V = 4\pi\varepsilon r_0^3 \tag{A11}$$

Thus, the molar volume expansion coefficients of the ABX₃ and ABY₃ are calculated as

$$\omega_{\text{ABX}_3} = \frac{4\pi\varepsilon N_a r_X^3}{V_X} = 3\frac{r_Y - r_X}{r_X} \text{ and } \omega_{\text{ABY}_3} = 3\frac{r_X - r_Y}{r_Y}$$
(A12)

under the condition that there is no overlapping of the strain fields introduced by the addition of solute atoms. If there exists overlapping of the strain fields introduced by the addition of solute atoms, the molar volume expansion coefficients of the ABX₃ and ABY₃ are less than the results calculated from equation (A12). Let λ_X and $\lambda_Y (\leq 1)$ be two positive parameters associated with the overlapping of the strain fields introduced by the addition of solute atoms, equation (A12) can be modified as

$$\omega_{\text{ABX}_3} = 3\lambda_X \frac{r_Y - r_X}{r_X} = \lambda_X \frac{V_Y - V_X}{V_X} \text{ and } \omega_{\text{ABY}_3} = \lambda_Y \frac{V_X - V_Y}{V_Y}$$
(A13)

It should be pointed out that numerical calculation, such as finite element method, is needed to determine the variation of both λ_X and λ_Y with the fraction of solute atoms in a solid solution.

ORCID iDs

Fuqian Yang https://orcid.org/0000-0001-6277-3082

References

[1] Docampo P and Bein T 2016 Acc. Chem. Res. 49 339 [2] Liu Y, Kim D, Ievlev A V, Kalinin S V, Ahmadi M and Ovchinnikova O S 2021 Adv. Funct. Mater. 31 2102793 [3] Tang X, Kothalawala N L, Zhang Y, Qian D, Kim D Y and Yang F 2021 Chem. Eng. J. 425 131456 [4] Lin C-H et al 2018 ACS Nano 13 1168 [5] Xia J X et al 2022 Joule 6 1689 [6] Chan K K, Giovanni D, He H, Sum T C and Yong K-T 2021 ACS Appl. Nano Mater. 49022 [7] Lian H et al 2022 Coord. Chem. Rev. 452 214313 [8] Arumugam G M, Karunakaran S K, Galian R E and Pérez-Prieto J 2022 Nanomaterials 12 2130 [9] Jain U, Soni S and Chauhan N 2022 Expert Rev. Mol. Diagn. 22 867 [10] Wang R, Huang T, Xue J, Tong J, Zhu K and Yang Y 2021 Nat. Photonics 15 411 [11] Li P, Jiang X, Huang S, Liu Y and Fu N 2021 Surfaces and Interfaces 25 101287 [12] Liu L, Xiao Z, Zuo C and Ding L 2021 J. Semiconduct. 42 020501 [13] Vashishtha P and Halpert J E 2017 Chem. Mater. 29 5965 [14] Zhang H C et al 2019 Nat. Commun. 10 1088 [15] Elmelund T, Seger B, Kuno M and Kamat P V 2020 ACS Energy Lett. 5 56 [16] Knight AJ et al 2021 ACS Energy Lett. 6799 [17] Hoke ET, Slotcavage DJ, Dohner ER, Bowring AR, Karunadasa HI and McGehee MD 2015 Chem. Sci. 6613 [18] Barker A J et al 2017 ACS Energy Lett. 2 1416 [19] Suchan K, Merdasa A, Rehermann C, Unger E L and Scheblykin I G 2020 J. Lumin. 221 117073 [20] Nandi P, Giri C, Swain D, Manju U, Mahanti S D and Topwal D 2018 ACS Appl. Energy Mater. 1 3807 [21] Brivio F, Caetano C and Walsh A 2016 J. Phys. Chem. Lett. 7 1083 [22] Shannon R D 1976 Acta Crystallographica section A 32 751 [23] Hu J G et al 2017 ACS Energy Lett. 2 950 [24] Zhang T et al 2017 J. Phys. Chem. Lett. 8 5069 [25] Han J S et al 2019 ACS Appl. Mater. Interfaces 11 8155 [26] Shaban A, Joodaki M, Mehregan S and Rangelow I W 2019 Org. Electron. 69 106 [27] Wang X et al 2017 Nano Lett. 17 4831 [28] Wang H, Zhou M and Luo H 2018 ACS Omega 3 1445 [29] Chen Y X et al 2019 J. Mater. Chem. A 7 20201 [30] Ullah S et al 2021 Energy Technology 9 2100691 [31] Porter D A and Easterling K E 2009 Phase Transformations in Metals and Alloys 3rd ed (CRC Press) [32] Hume-Rothery W 1969 Indian J. Phys. 11 74 [33] Wert C and Zener C 1949 Phys. Rev. 76 1169 [34] Zener C 1949 Acta Crystallogr. 2 163 [35] Machlin E 1954 JOM 6 592 [36] Oriani R 1956 Acta Metall. 4 15 [37] Li J, Oriani R and Darken L 1966 Z. Phys. Chem. 49 271 [38] Myhill R 2018 Contrib. Mineral. Petrol. 173 12 [39] Yang F 2006 J. Appl. Phys. 99 054306 [40] Yao Y, Cheng C, Zhang C, Hu H, Wang K and De Wolf S 2022 Adv. Mater. 34 2203794 [41] Li Q et al 2022 Adv. Energy Mater. 12 2202982 [42] Sher A, van Schilfgaarde M, Chen A-B and Chen W 1987 Physical Review B 36 4279 [43] Faghihnasiri M, Izadifard M and Ghazi M E 2017 The Journal of Physical Chemistry C 121 27059 [44] Slotcavage D J, Karunadasa H I and McGehee M D 2016 ACS Energy Lett. 1 1199 [45] Tang X F et al 2018 Nano Lett. 18 2172

[48] Flynn C P 1972 Solid State Processes: Point Defects and Diffusion. (Oxford University Press)

[46] Ni X et al 2019 Nanotechnology 30 165402
 [47] Yang F Q 2023 Solid State Commun. 371 115244

[49] Eshelby J 1954 J. Appl. Phys. 25 255